EUROPEAN JOURNAL OF BIOMEDICAL AND PHARMACEUTICAL SCIENCES

http://www.ejbps.com

ISSN 2349-8870
Volume: 10
Issue: 8
183-190
Year: 2023

BIOSYNTHESIS OF PRISTINE ZNO AND CO-DOPED ZNO NANOCOMPOSITES USING MENTHA PIPERITA LEAF EXTRACT FOR PHOTOCATALYTIC AND ANTIOXIDANT APPLICATIONS

S. Malathi[a], G. Myvizhi[b]* and K. Vanitha Bharathi[c]

[a,b]Department of Chemistry(PG), Vellalar College for Women,Erode-638 012, Tamilnadu, India.
[c]Department of Chemistry, Vellalar College for Women,Erode-638 012, Tamilnadu, India.

***Corresponding Author: Prof. G. Myvizhi**
Department of Chemistry(PG), Vellalar College for Women,Erode-638 012, Tamilnadu, India.

Article Received on 24/05/2023 **Article Revised on 14/06/2023** **Article Accepted on 04/07/2023**

ABSTRACT
The purpose of this work is the preparation of ZnO Nanocatalyst doped with TiO_2 and Ag to treat the industrial effluent by the method of photocatalytic degradation under the visible light. ZnO is one of the excellent photocatalysts for the complete degradation of organic contaminants in the effluent which is low cost, availability and non-toxic. But the band gap of ZnO is high around 3.2 eV so the dopant like TiO_2 and Ag is introduced to improve the photocatalytic activity. The synthesis of Photocatalyst is done by green synthesis method and the samples were characterised by various techniques. The doped catalyst is set to react with the Methylene blue. Absorbance and Reaction time are the two main factors that improved the decolorization and degradation was observed and the actual wavelength for the Methylene Blue were analysed under the UV spectrometer. The initial value will be compared with the final value.

KEYWORDS: Green Synthesis, ZnO Nanoparticles, Photocatalytic activity, Methylene Blue, antioxidant.

1. INTRODUCTION
ZnO NPs have captured the interest of numerous researchers in recent years due to their distinctive optical and chemical behaviours, which can be easily modified by altering the shape. ZnO NPs, a member of the large family of metal oxide nanoparticles, are employed in a variety of cutting-edge applications, including those in the fields of electronics, communication, sensors, cosmetics, environmental protection, biology, and medicine.[1] Along with its antibacterial, antifungal, acaricidal, pediculicidal, larvicidal, and anti-diabetic actions, ZnO NP has enormous potential in biological applications such as biological sensing, biological labelling, gene transport, drug delivery, and nanomedicine.[2-5] Researchers have recently begun to choose environmentally friendly methods of creating NPs since they are inexpensive, can be created in ambient air, are non-toxic, compatible with the environment, and are simple to use because the produced particles are highly uniform[6-8] Numerous researchers have become interested in ZnO NPs in recent years because to its unique optical and chemical behaviours, which can be easily changed by changing the form. A range of cutting-edge applications, including those in the sectors of electronics, communication, sensors, cosmetics, environmental protection, biology, and medicine, use ZnO NPs, a member of the broad family of metal oxide nanoparticles.[9] ZnO NP has significant promise in biological applications such biological sensing, biological labelling, gene transport, drug delivery, and nanomedicine. These biological applications include antibacterial, antifungal, acaricidal, pediculicidal, larvicidal, and anti-diabetic properties.[10] Due to their low cost, ability to be produced in ambient air, lack of toxicity, compatibility with the environment, and ease of use, researchers have recently started to pick environmentally benign methods of producing NPs. Due to its low temperature fabrication, less contamination, and increased photocatalytic activity, sol-gel is still the most straightforward approach for synthesising TiO_2 and ZnO as films or nanopowders.[11] A versatile and efficient process, photocatalysis can be tailored to match a variety of applications for disinfection in both water and air matrices. Nevertheless, photocatalytic surfaces are being created and approved for use in goods with the designation "self-disinfection."[12] TiO_2 was modified by adding another metal oxide-based semiconductor in a variety of ways, including dye sensitization, metal- or non-metal-doped TiO_2-based nanostructures, and metal- or non-metal-doping TiO_2. These modifications made TiO2 effective in absorbing solar energy in a wide spectrum from UV to visible. There is evidence that coupled semiconductors make efficient and effective photocatalysts.[13] Theoretically,

the pairing of different semiconductor oxides tends to be advantageous for processing a wide range of solar energy (both ultraviolet and visible regions) and for achieving more effective electron-hole pair separation, leading to the achievement of a higher photocatalytic operation.[14] Numerous composites made of TiO_2 and other inorganic oxides have been found, including ZnO, SnO_2, SiO_2, In_2O_3, Cu_2O, MgO, WO_3, and MoO_3.

One of the most well-known herbal teas with only one ingredient is peppermint tea (Mentha piperita), which is prized for its revitalising flavour and aroma. It is a perennial herb that is indigenous to Europe and has spread into many other nations, including the northern United States and Canada.[15] With a focus on NP development at various temperatures, we created ZnO NPs that were codoped with TiO_2 and Ag throughout our research using green methods using MP leaf extract. This is the first time MP leaf extract has been used as a reducing and stabilising agent in an environmentally friendly way to prepare Ag/ZnO nanocomposite.[16] The reduction of methyl orange (MO) by an Ag/ZnO nanocomposite and its catalytic activity.[17]

2. MATERIALS AND METHODS

2.1 Materials

The following chemicals, which were purchased from the chemical company, were used in the hydrothermal method to create the proposed title composite materials: titanium isopropoxide ($C_{12}H_{28}O_4Ti$), silver nitrate ($AgNO_3$), zinc acetate ($ZnC_4H_6O_4$), 0.1 M aqueous NaOH solution, and double-distilled water from Mentha piperita (MP) plant leaves.

2.2. Plant extracts preparation

5 g of Mentha piperita leaves were properly cleaned with lots of distilled water before being gently rubbed with alcohol to sterilise both surfaces. In 100 cc of distilled water heated to 50 C, these leaves were heated for 30 minutes. The extract was then filtered using Whatman filter paper No. 1 and a vacuum filter with 0.2 mm pore size. The finished filtrate was kept in a cool, dry location for later use.

2.3 Synthesis of Pristine ZnO, TiO_2/ZnO, Ag/ZnO Nanocomposites

Green MP leaf extract was used to prepare zinc oxide nanoparticles. Using a weighing scale, 20 g of zinc acetate dihydrate and 80 g of sodium hydroxide were weighed for the preparation. Then, 80 g of sodium hydroxide was dissolved in 100 mL of distilled water, and 20 g of zinc acetate dihydrate was dissolved in 150 ml of distilled water. For approximately five minutes each, the solutions were agitated continuously with MP leaf extract. After thoroughly combining, a solution of sodium hydroxide was added to the zinc acetate solution while being continuously stirred with a magnetic stirrer for about five minutes. Then, a burette was filled with 100 ml of ethanol and titrate drop wise to the solution containing both sodium hydroxide solution and zinc acetate. After the reaction, white precipitate was formed, which is calcined and powdered ZnO is prepared. The doped TiO_2/ZnO, Ag/ZnO can be prepared by the same method (Fig 1).

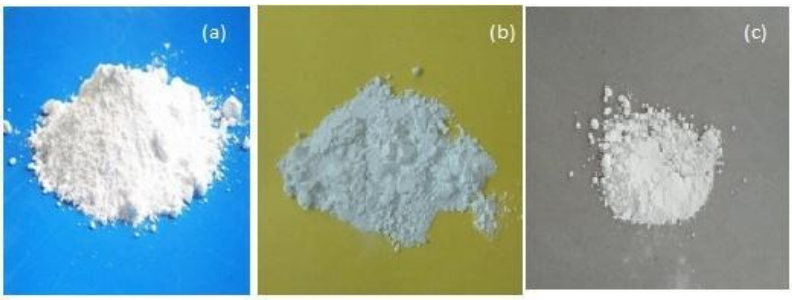

Fig. 1: Images of a) ZnO NPs b) TiO2/ZnO NCs c) Ag/ZnO NCs.

2.4 Characterization

Characterization of NPs had been done by X-ray diffraction (XRD) and Fourier transformed infrared spectroscopy (FTIR). Morphology of prepared samples was analysed by field emission scanning electron microscopy (FESEM) and high resolution transmission electron microscopy (HRTEM) was used to investigate the particle size. Anti-bacterial assay has been performed. Anti-diabetic activity was also investigated suggesting probable mechanisms for their potential medicinal uses. Induction of cytokines and other regulatory genes associated with diabetes had been studied in response to ZnO treatments in animal models utilising ELISA and RT-PCR techniques.

2.5 Photocatalytic activity

The following procedure was used to determine the photocatalytic activities of the as-prepared catalysts (ZnO, TiO_2/ZnO, Ag/ZnO) on the degradation of methyl blue dye in an aqueous solution under visible light. The degradation pool typically consists of a 50 ml methylene blue (MB) aqueous solution (50 ppm), and with that, 0.5 g of the as-prepared nanomaterial was blended in the same beaker. The blended solution was shocked in the darkroom for 60 min and adjusted its pH level to different values (4, 6 and 8) by using NaOH solutions before ultraviolet ray irradiation to achieve adsorption/desorption equilibrium. After that, the solution was exposed to visible light under constant stirring. At regular intervals, a specific mixture solution

(5 ml) was collected and filtered via a syringe filter. Eventually, the breakdown of methylene blue was investigated by using a UV-7504 PC to determine the absorption at 642 nm (CANY Shanghai). To replicate the solar spectrum, a xenon lamp (50 W, CEL-HXF300) was employed.[18]

2.6 Antioxidant activity –DPPH assay

The Liyana-Pathiranan and Shahidi method was used to conduct the DPPH free radical scavenging experiment. To 1 mL of 0.135 mM DPPH in methanol solution, varied quantities of the synthesised Zno NPs and aqueous leaf extract (100–500 mg in methanol) were added. The reaction mixture was kept at room temperature for 30 minutes in the dark. At 517 nm, absorbance was determined spectrophotometrically.[19]

3. RESULTS AND DISCUSSION

3.1 XRD analysis

The X-ray diffraction pattern of the synthesis ZnO nanorods and ZnO nanoflakes is displayed in Fig.2(a). The exceptional quality of the synthetic ZnO nanorods is demonstrated by the strong and distinct diffraction peaks. The hexagonal structure of ZnO with fine crystallinity can be indexed to all of the diffraction peaks in the XRD pattern.The ZnO planes (100), (002), (101), (102), (110), (103), (112), and (201) are respectively indexed to the diffraction peaks at 2° (degree) of 31.76, 34.43, 36.267, 47.569, 56.62, 62.88, and 69.12. Applying the relation, the lattice parameters have been derived.

$$1/d^2 = 4/3[(h^2 + hk + k^2 / a^2)] + l^2 / c^2$$

The calculated values, a=3.248 Å and c=5.215, Å match well with the stated standard values, a=3.249 Å and c=5.206 Å (JCPDS no. 36-1451). Using the semi-empirical formula D=k / cos, Scherer's average particle size (D) is derived. Where is the full width at half maximum (FWHM), 1.5406 is the X-ray wavelength, 0.94 is the form factor, and is the Bragg angle in degrees. Using an XRD pattern processing programme, profile fitting was used to determine the value of FWHM.[20]

The calculated values are a=3.248 Å and c=5.215 Å, the values are in good agreement with the reported standard values a=3.249 Å and c=5.206 Å (JCPDS no. 36-1451). The average particle size (D) are calculated using the Scherer's semi empirical formula D= k λ / β cosθ Where λ is the wavelength of the X-ray (1.5406 Å), k is the shape factor ($\approx$ 0.94), β is the full width at half maximum (FWHM) and θ is the Bragg angle (degree). The value of FWHM was obtained by performing profile fitting using an XRD pattern processing software. It was determined that the typical crystallite size was 31 nm. According to Fig. 2(b), ZnO nanoparticles and TiO2 have diffraction peaks that are present at 2 (degree) of 27.900, 40.451, and 50.602 on average in the (101), (200), and (004) diffraction planes that correspond to TiO2 (JCPDS No. 36-1451).[21] The majority of the diffraction peaks in the XRD pattern are also crisp, symmetrical Gauss peaks, which is yet another sign of the great crystallinity of the TiO_2 and ZnO particles in the composite samples. The outcomes are also linked to other studies.Additionally, Fig.2c reveals that the Ag/ZnO XRD pattern exhibits several additional reflections at 2 = 38.1°, 44.4°, 64.9°, and 77.2°, which correspond to the (111), (200), (220), and (311) reflections of the face-centred cubic silver NPs (JCPDS 870717) immobilised on the surface of the ZnO.[22]

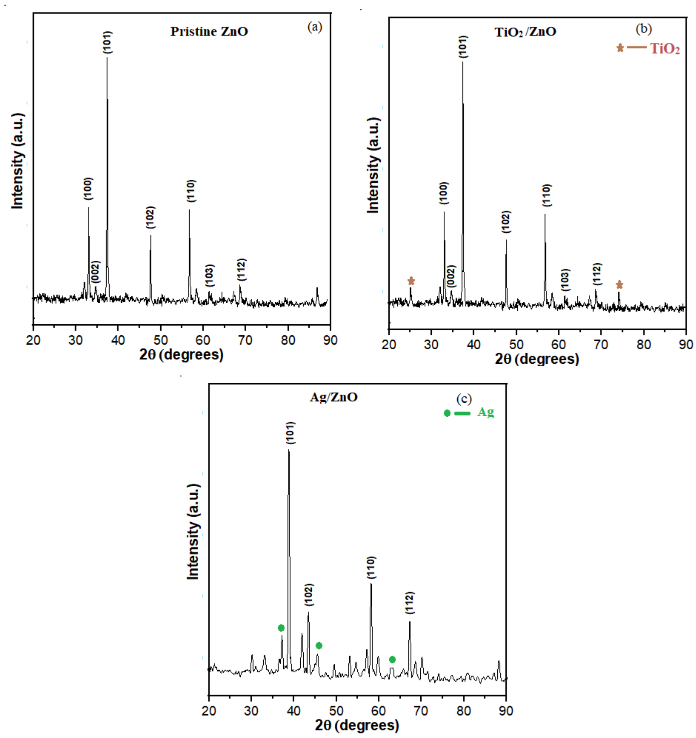

Fig. 2: XRD images of (a) ZnO (b) TiO_2/ZnO (c)Ag/ZnO nanocomposites.

3.2 SEM analysis

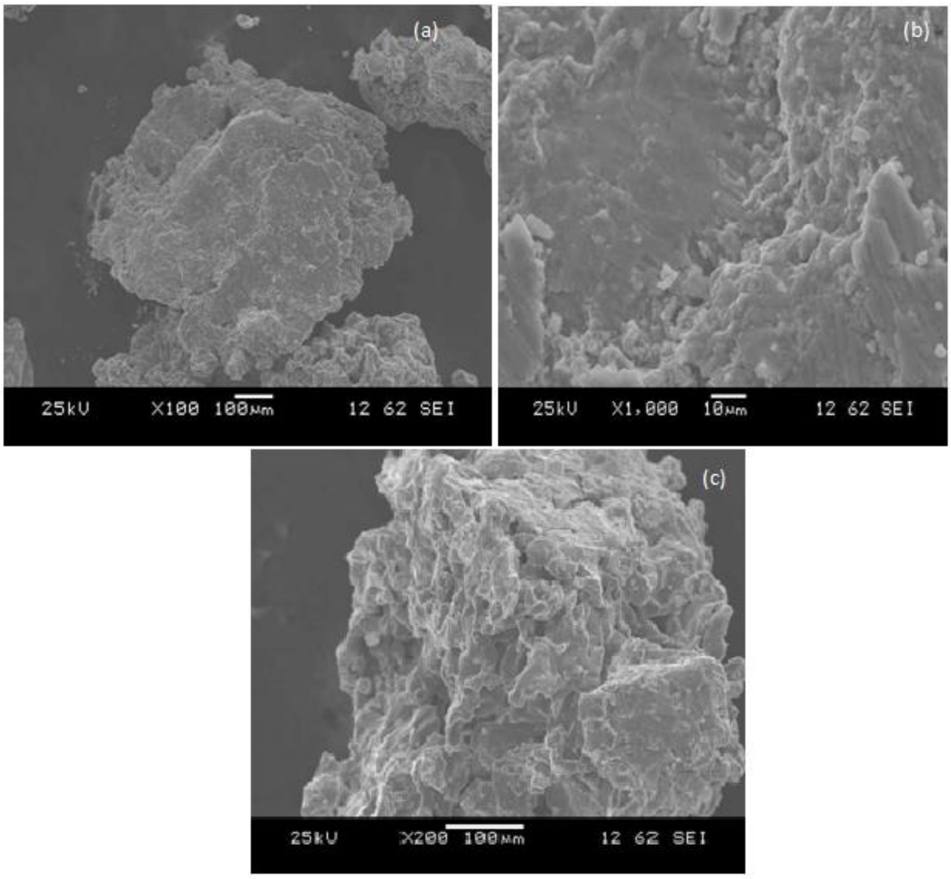

Fig. 3: SEM images of pristine (a) Zno NPs b) TiO2/ZnO NCs c) Ag/ZnO NCs.

The SEM micrographs of the nanoparticles created using MP leaf extract are shown in Fig.3a. According to a topographical view, the aggregates' surfaces appear to be rough and the nanoparticles appear to be grouped together. It can be inferred from SEM pictures that the green method's nanoparticles are fully clean and that the plant extract has a remarkable capacity for ZnO NP synthesis.

The effective preparation of ZnO nanoparticles has crystallite sizes ranging from 8 mm to 40 nm. The product made using the green approach allowed for the observation of the changed precursor's effect.[23] It has been unequivocally established from the SEM pictures that the synthesised TiO_2/ZnO powder is in nanoscale form. As shown in Fig. 3b, the particle size of the synthetic TiO_2/ZnO powder is approximately 84.98 nm. The SEM result, which showed that the synthesised TiO_2/ZnO nano-powder exhibits good crystallinity, is consistent with this outcome. It is regarded as a successful outcome because the synthesised TiO_2/ZnO particle size is less than 100 nm. Additionally, ZnO particles were widely scattered on the surfaces of the produced TiO_2 bulks, which would be advantageous to enhance the catalytic activity of the TiO_2/ZnO composite photocatalysts in general. TiO_2 particles are the primary constituents of the TiO_2/ZnO composite samples. Additionally, the samples contain small amounts of aggregated nanoscale particles made from TiO_2 and ZnO crystalline grains.[24]

The findings in Fig. 3c show that silver nanoparticles are mono-dispersive, highly crystalline, and spherical in appearance.[25] The samples acquired from the SEM image have greater grain sizes. This indicates that the high surface energy and high surface tension of the Ag/ZnO nanoparticles contribute to their propensity to aggregate. A larger surface is produced by the finer particle size.[26] The catalytic activity of nanoparticles is improved by area.

3.3 FTIR analysis

The analysis and results of the FTIR spectra of the as-prepared ZnO, TiO_2/ZnO, and Ag/ZnO nanocomposites are shown in Fig.4. The transmissions at 506 and 561 cm^{-1} were shown in Fig.4a. It was discovered that these transmissions were caused by a symmetric bending vibration of Zn-O in the ZnO NPs and TiO_2/ZnO NCs, respectively.[27] The presence of bands at 1591 cm^{-1} or 3581 cm^{-1}, which correspond to the surface H-OH bending vibration and O-H stretching vibration, respectively, indicates that there was hydroxyl-group adsorption on the ZnO surface, resulting in ZnO production. The stretching bond of Zn-O-Ti and Ti-O-C exhibited in Fig.4b corresponds to the peak seen at 829 cm^{-1} and 1384 cm^{-1}.[28] The distinctive peaks of ZnO and Ti-O were also visible in the overlapped form in TiO_2-

and Ag-loaded ZnO composite. There is no evidence for the formation of Ag–O. Hence it could be a metallic silver (Ag-Zn-O) present in the nanocomposites.

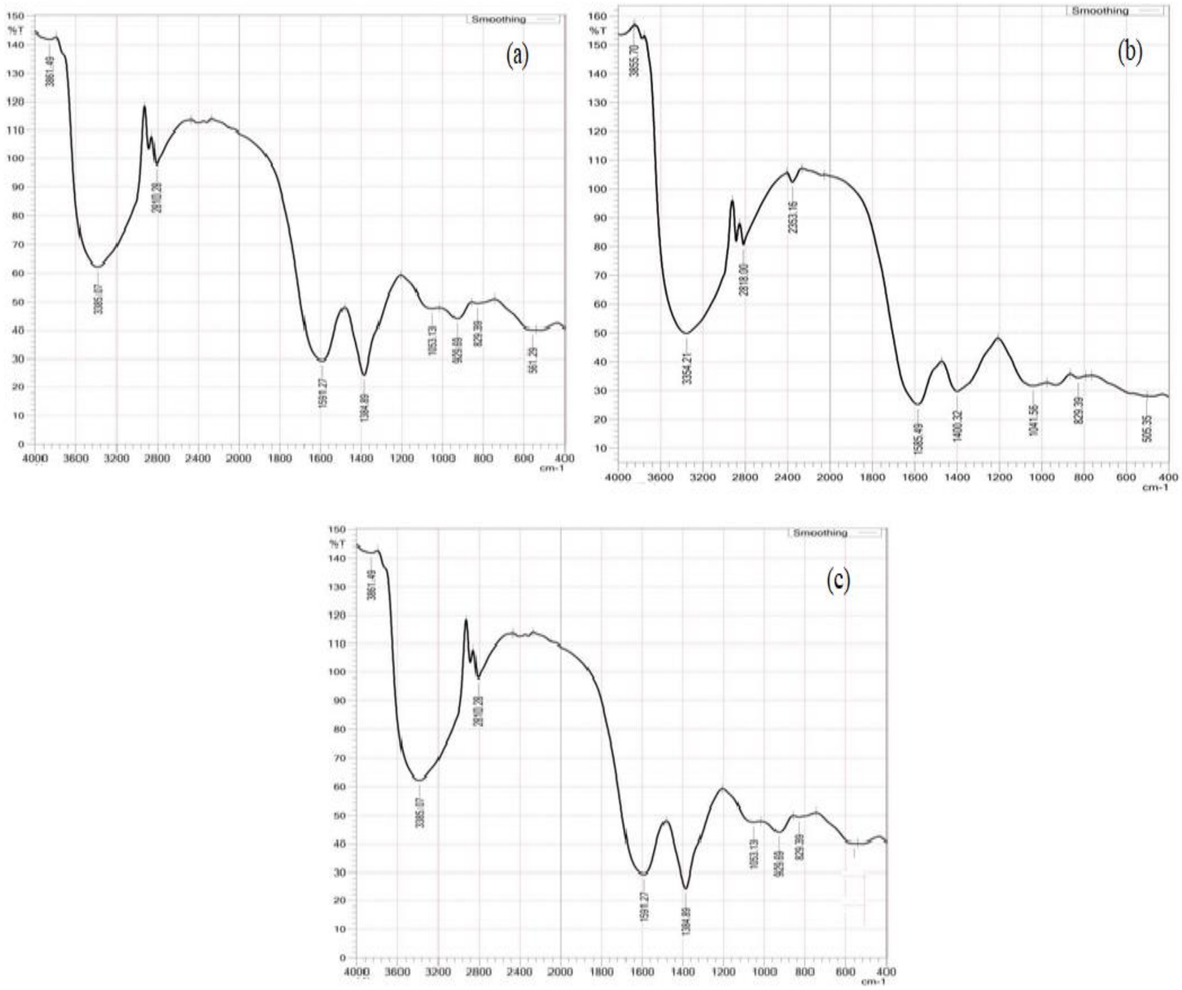

Fig. 4: FTIR images of pristine (a) Zno NPs b) TiO2/ZnO NCs c) Ag/ZnO NCs.

3.4 Photocatalytic degradation of methylene blue dye

The utilisation of ZnO NP, TiO_2/ZnO, and Ag/ZnO NCs for photocatalytic activities is influenced by the optical absorption in the UV region and corresponding photo efficiency. By degrading 10 ppm of MB at pH=6, the photocatalytic activity of ZnO, TiO_2/ZnO, and Ag/ZnO NCs was assessed. The impact of the catalyst's irradiation period on the methylene blue absorbance for ZnO, TiO_2/ZnO, and Ag/ZnO NPCs is shown in Fig.4(a). It is evident that increasing the catalyst's irradiation period from 1 hour,2 hour, 3 hour and 4 hour causes the first slopes of the curves depicting the rate of absorbance to rise significantly.

The comparison of all the molar concentrations of ZnO particles produced using the green approach is shown in Fig. 4, and it is evident from this comparison that the 1:0.1 M concentration results in the highest photocatalytic activity. In contrast to ZnO and TiO_2/ZnO NPCs, the ZnO /Ag NPCs created using the green approach exhibit increased catalytic activity, as shown by the figure. The development of nano composites during green synthesis may be the cause. Ag/ZnO nanocomposites' improved catalytic performance is mostly attributable to their increased surface area than other structures, which may also be the cause of their improved catalytic activity. As a result, the ZnO NPs surface produces more negative surface charges, which easily bind and destroy the methylene blue molecule. Positive surface charge on the surface of the ZnO is the cause of the low degradation of methylene blue by the material. Since methylene blue is a cationic dye, the positive charge on the ZnO surface does not pay attention to attract the molecule.[29]

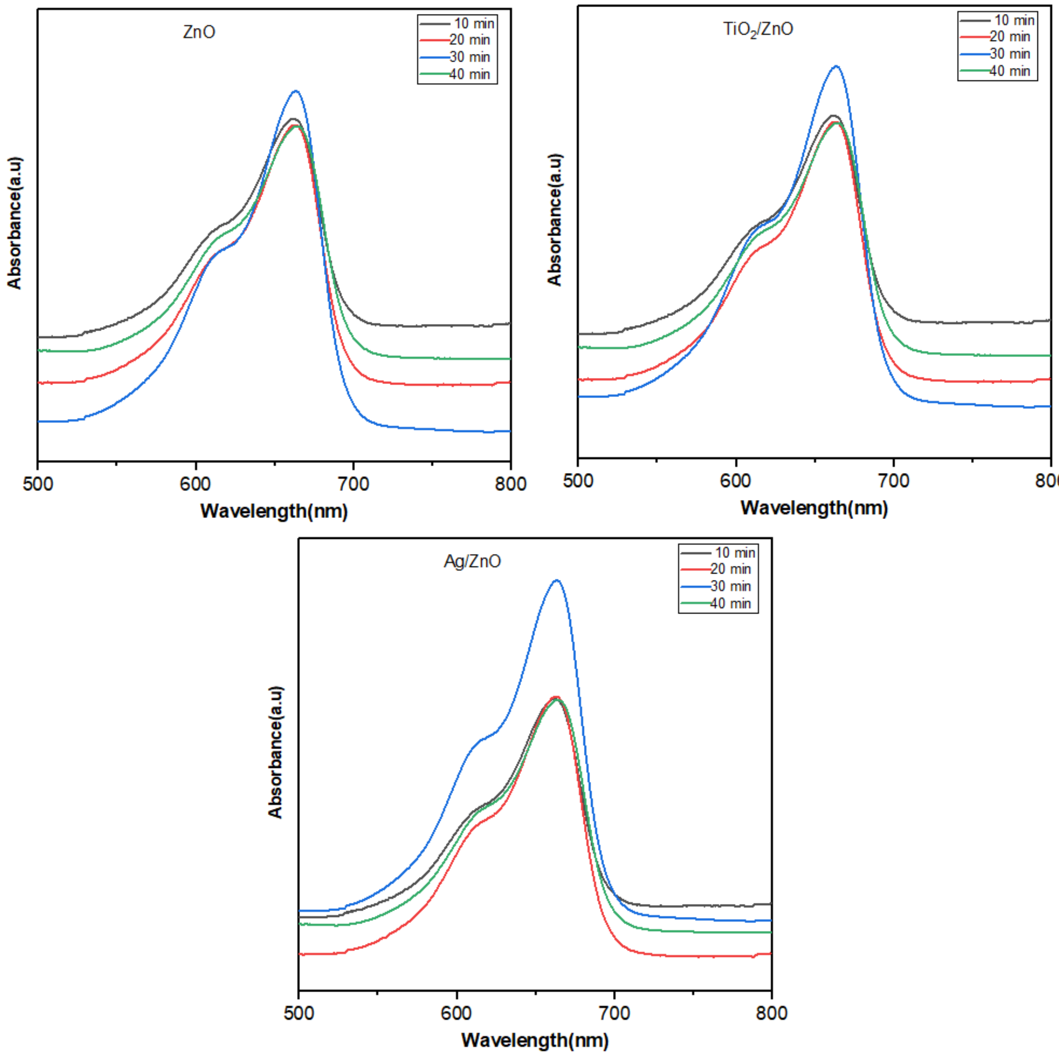

Fig. 5: Photocatalytic degradation of pristine (a) Zno NPs b) TiO_2/ZnO NCs c) Ag/ZnO NCs against methylene blue.

3.5 Antioxidant Activity

The substance known as an antioxidant shields cells from harm caused by free radicals. The DPPH approach is a rapid, accurate, and extremely promising way to find out whether the produced nanoparticles have any antioxidant properties. Antioxidants scavenged the DPPH radical by donating a proton to generate the reduced DPPH [30]. The decline in absorbance at wavelength 517 nm can be used to measure the colour change from purple to yellow after reduction. Fig.6. compares and displays the antioxidant activity of pure ZnO, TiO_2/ZnO, and Ag/ZnO nanoparticles. It was discovered that increasing the dose concentration from 100 to 500 g/ml enhanced the antioxidant property of the nanostructures as-prepared. In comparison to pure ZnO (50.630.50) and TiO_2/ZnO (54.200.90), Ag/ZnO showed high inhibitory properties at the highest concentration of 500 g/ml, 58.100.20%. The nanoparticles in order of their antioxidant capacity are MP-Ag/ZnO, MP-TiO_2/ZnO, MP-ZnO, and Pure ZnO. Hence higher antioxidant properties are shown by the MP-Ag/ZnO nanocomposites, which may provide an option in nanomedicine.

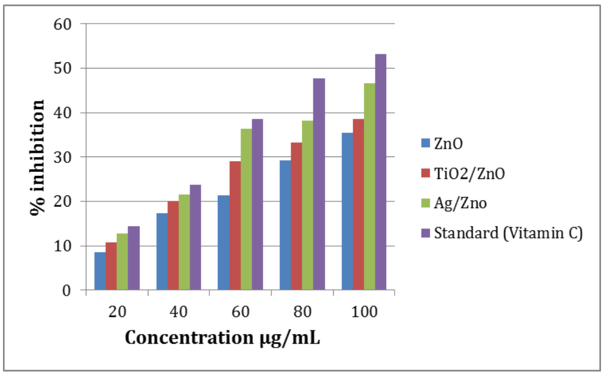

Fig. 6: Antioxdant activity of Synthesised nanocomposites.

4. CONCLUSION

Ag and TiO_2 co doped ZnO nanocomposites physiochemical characteristics as well as their photocatalytic activity were investigated in this study. The sizes of the newly formed crystalline nanostructures were between 13, 15, and 16 nm. By using FTIR analysis, their functional groups which match the XRD spectrum were discovered. According to surface and morphological studies, Ag-loaded TiO_2 has a spherical shape, while the remaining particles are clustered nanoparticles. Subsequently, the Ag/ZnO nanocomposite outperformed other nanocomposites at pH 6 because of its photocatalytic behaviour, which showed a greater degradation ratio. Ag/ZnO nanocomposite also showed increased performance in terms of antioxidant activity when compared to pure and TiO_2 loaded ZnO nanostructures.

REFERENCES

1. C. Dagdeviren, S. W. Hwang, Y. Su, S. Kim, et al. Transient, Biocompatible Electronics and Energy Harvesters Based onZnO, Small, 2013; 9(20): 3398–3404.
2. H. M. Xiong, ZnO Nanoparticles Applied to Bioimaging and Drug Delivery, Adv. Mater., 2013; 25(37): 5329–5335.
3. D. Sharmaa, J. Rajputa, B. S. Kaitha and M. Kaurb, Synthesis of ZnO nanoparticles and study of their antibacterial and antifungal properties, Thin Solid Films, 2010; 519(3): 1224–1229.
4. A. Alkaladi, A. M. Abdelazim and M. A, Antidiabetic Activity of Zinc Oxide and Silver Nanoparticles on Streptozotocin-Induced Diabetic Rats, Int. J. Mol. Sci., 2014; 15: 2015–2023.
5. J. Qu, X. Yuan, X. Wang and P. Shao, Zinc accumulation and synthesis of ZnO nanoparticles using Physalis alkekengi L, Environ. Pollut., 2011; 159(7): 1783–1788.
6. Ameta, R., Solanki, M.S., Benjamin, S. and Ameta, S.C., Photocatalysis. In:Advanced Oxidation Processes for WasteWater Treatment. London: Elsevier, 2018; 135-175.
7. Aminuzzaman, M. et al., Value-adding to dragon fruit (Hylocereus polyrhizus)peel biowaste: green synthesis of ZnO nanoparticles and their characterization. Inorganic and Nano-Metal Chemistry, 2019; 49(11): 401-411.
8. Gour, A. and Jain, N.K., Advances in green synthesis of nanoparticles. Artificial cells, Nanomedicine, and Biotechnology, 2019; 47(1): 844-851.
9. McKay, D.L. and Blumberg, J.B., A review of the bioactivity and potential health benefits of peppermint tea (Mentha piperita L.). Phytotherapy Research, 2006; 20: 619-633.
10. Nadaroğlu, H., Alayli A.., Synthesis of Nanoparticles by Green Synthesis Method. International Journal of Innovative Research and Review, 2017; 1(1): 6-9.
11. Rita, P. and Animesh, K., An updated overview on peppermint (Mentha piperita). International Research Journal of Pharmacy, 2011; 2(8): 1-10.
12. Shkurupii, V.A., Odintsova, O.A. and Kazarinova, N.V., Use of essential of peppermint (Mentha piperita) in the complex treatment of patients with infiltrative pulmonary tuberculosis. Problemy Tuberkuleza i Bolezneĭ Legkikh, 2006; 9: 43-45.
13. Atarod, M., Nasrollahzadeh, M., Sajadi, S.M.: 'Euphorbia heterophylla leaf extract mediated green synthesis of Ag/TiO2 nanocomposite and investigation of its excellent catalytic activity for reduction of variety of dyes in water', J. Colloid. Interface Sci., 2016; 462: 272–279.
14. Dodoo-Arhin D, Buabeng FP, Mwabora JM, Amaniampong PN, Agbe H, Nyankson E, et al. The effect of titanium dioxide synthesis technique and its photocatalytic degradation of organic dye pollutants. Heliyon, 2018; 4(7): e00681.
15. Wang C, Xu B-Q, Wang X, Zhao J. Preparation and photocatalytic activity of ZnO/TiO2/SnO2 mixture. J Solid State Chem., 2005; 178(11): 3500–6.
16. Hatamifard,A., Nasrollahzadeh, M., Sajadi, S.M.: 'Biosynthesis, characterization and catalytic activity of an Ag/zeolite nanocomposite for base- and ligand-free oxidative hydroxylation of phenylboronic acid and reduction of a variety of dyes at room temperature', New J. Chem., 2016; 40: 2501–2513.
17. Rizzo L, Meric S, Guida M, Kassinos D. Belgiorno V. Heterogenous photocatalytic degradation kinetics and detoxification of an urban wastewater treatment plant effluent contaminated with pharmaceuticals. Water Research, 2009; 43(16): 4070-8. Ashwini Jayachandran, Aswathy T.R., Achuthsankar S. Nair, Green synthesis and characterization of zinc oxide nanoparticles using Cayratia pedata leaf extract, Biochemistry and Biophysics Reports, July, 2021; 26.
18. Dr. Keshav k Deshmukh, Goraksh J. Hase, Tukaram R. Gaje, Narendra D. Phatangare, Ghumare Shilpa, Varpe Ashwini, "Titanium Oxide Nanoparticles and Degradation of Dye by Nanoparticles", International Journal of Material Science, 2018; 13(1): 23-30.
19. Tran Manh Cuong, Vu Anh Tuan, Dang Tuyet Phuong, Tran Thi Kim Hoa, Bui Hai Linh & Masakazu Anpo, "Novel method for doping nano TiO photocatalysts by chemical vapour deposition", Journal of Experimental Nanoscience, 2012; 7(1): 42-52.
20. Vilar VJP, Gomes AIE, Ramos VM, Maldonado MI, Boaventura RAR. Solar photocatalysis of a recalcitrant coloured effluent from a wastewater treatment plant Photochemical & Photobiological Sciences, 2009; 8(5): 691-8.
21. Ni M, Leung MKH, Leung DYC, Sumathy K. A review and recent developments in photocatalytic water-splitting using TiO; for hydrogen production. Renewable and Sustainable Energy Reviews, 2007; 11: 401-25.
22. Samanamud GRL, Loures CCA, Souza AL, Salazar RFS, Oliveira IS, Silva MB, et al. Heterogeneous photo catalytic degradation of dairy 48 wastewater using immobilized ZnO. ISRN Chemical Engineering, 2012; 275371: 18.
23. Zhang S, Chen Z, Li Y, Wang Q, Wan L. Photocatalytic degradation of methylene blue in a sparged tube reactor with TiO2 fibers prepared by a

properly two-step method. Catalysis Communications, 2008; 9: 1178-1183.
24. Saleh TA, Gondal MA, Drmosh QA, Yamani ZH, AL-yamani A. ZnOnano particles on multiwall carbon nanotubes. Chemical Engin J., 2011; 166: 407-412.
25. Rajeev KW, William W, Liu Y, Michelle LM, Joshua CF, et al. Photodegradation of Congo Red catalyzed by nanosized TiO2. Journal of Molecular Catalysis A: Chemical., 2005; 242: 48-56.
26. Bandekar, G., Rajurkar, N. S., Mulla, I. S., Mulik, U. P., Amalnerkar, D. P. and Adhyapak, P. V. Synthesis, characterization and photocatalytic activity of PVP stabilized ZnO and modified ZnO nanostructures. Applied Nanoscience, 2013; 4(2): 199-208.
27. Hairom, N. H. H., Mohammad, A. W. and Kadhum, A. A. H. Effect of various zinc oxide nanoparticles in membrane photocatalytic reactor for Congo red dye treatment. Separation and Purification Technology, 2014; 137: 74-81.
28. M.T. Amin, A.A. Alazba and U. Manzoor, "A Review of Removal of Pollutants from Water/Wastewater Using Different Types of Nanomaterials" , Hindawi Publishing Corporation, Article ID 825910, 2014; 2014: 24.
29. Prachi, Pranjali Gautam, Deepa Madathil, A.N. Brijesh Nair, "Nanotechnology in Waste Water Treatment: A Review ", International Journal of ChemTech Research, 2013; 5: 2303-2308.